Large-Scale Effects of Deep Convection on the GATE Tropical Boundary Layer

RICHARD H. JOHNSON

Department of Atmospheric Science, Colorado State University, Fort Collins 80523

(Manuscript received 20 February 1981, in final form 11 June 1981)

ABSTRACT

The large-scale response of the atmospheric boundary layer to the passage of tropical wave disturbances is investigated. Observations from GATE indicate that during periods of extensive deep convective activity rather shallow mixed layers frequently are found, primarily in association with mesoscale precipitation systems. Convective-scale precipitation downdrafts accompanying such systems contribute to the formation of large trailing "wakes" wherein there exist considerably enhanced fluxes of sensible heat from the ocean surface. Observations in the convectively active trough portion of tropical waves indicate that a considerable fraction of the total area is covered by wakes. However, there remain regions between rain systems in the wave trough covering ~15–30% of the total area, depending on how these regions are defined, which have mixed layers more characteristic of those observed in the undisturbed ridge portion of the wave than those in wakes.

A simple model is developed to study the maintenance of the mixed layer in regions between wakes. In the model, horizontal and vertical boundaries of the well-mixed layer are treated as zero-order discontinuities. The model takes into account, in a large-scale sense, the convergence of relatively cool downdraft air into the region between convective systems or wakes. Variables at the top of the mixed layer are specified using large-scale rawinsonde observations and a diagnostic model for the cloud layer above. Application of the model to a composite of a number of GATE wave disturbances has shown that during periods of abundant deep convective activity, environmental subsidence (subsidence away from cumulus and mesoscale downdraft systems) is weak and yet the mixed layer there does not grow without bound because of the inversion-strengthening effect of cool downdraft air outflow into the between-cloud region. Although the model is not fully closed, in the sense that a budget is not carried out to determine thermodynamic properties of downdraft air near the ground, it does suggest that large-scale numerical prediction models may be able to carry the mixed layer height as a predicted variable even during convectively disturbed situations.

1. Introduction

The structure and properties of the GATE (GARP Atlantic Tropical Experiment) atmospheric boundary layer have been investigated in a number of recent studies (Brümmer, 1978; Emmitt, 1978; Gaynor and Mandics, 1978; Gaynor and Ropelewski, 1979; Jalickee and Ropelewski, 1979; Barnes *et al.*, 1980; Nicholls and Le Mone, 1980). Considerable attention has been given in several of these studies to the pronounced modification or transformation of the boundary layer accompanying the onset of deep convective activity. The changes, occurring over a wide range of time and horizontal space scales, are often quite complex. Frequently, during disturbed periods observations show that in the wake of mesoscale precipitating systems, which are rather common in the GATE region (Leary and Houze, 1979), very shallow mixed layers (~200 m deep or less) persist over large areas for a considerable length of time, up to 12 h or longer. The source of the air in these layers, at least in part, is in precipitation downdrafts that originate in the low to mid-troposphere (Zipser, 1977).

The presence of significant mesoscale and smaller-scale variations in the tropical boundary layer during periods of deep convective activity makes the problem of parameterizing boundary layer structures in large-scale prediction models difficult. In particular, models that predict properties of the boundary layer and the mixed-layer depth (e.g., Arakawa and Schubert, 1974, and others) must, in light of the above studies, take into account the significant modification of the boundary layer in convective regions by precipitation and downdrafts (see also Betts, 1976a). Convective parameterization schemes that contain simple cloud models must be properly coupled with models for the mixed layer to include downdraft effects. It is one purpose of this paper to establish a theoretical framework for a properly coupled mixed layer–cloud layer model used in a diagnostic application of a particular parameterization theory (Arakawa–Schubert).

Another objective is to explain the relationship

0022-4928/81/112399-15$07.75

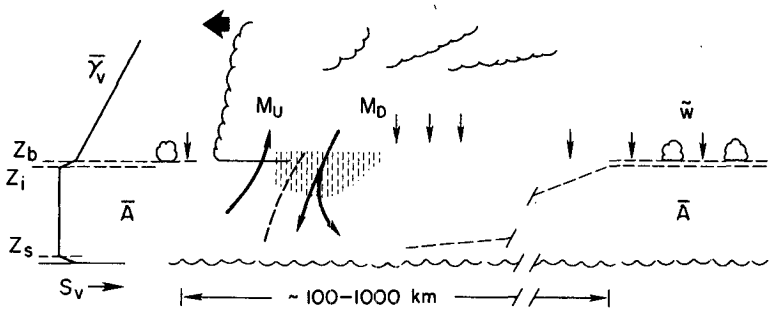

FIG. 1. Schematic of boundary layer in the vicinity of mesoscale convective systems. In region $\bar{A}$ away from convection the boundary layer is assumed to be well mixed. M_U and M_D denote updraft and downdraft mass fluxes. Other symbols are defined in text. Many convective systems have "wakes" much smaller than that shown here and the same model is assumed to qualitatively apply to those. The subsidence $\tilde{w}$ surrounding convective drafts determined by the cloud-layer diagnostic model is assumed horizontally uniform and applies to the area $\bar{A}$ as well as the portions of wakes away from deep convective drafts.

between the observed variation of the mixed-layer depth in tropical disturbances and the large-scale environmental subsidence at cloud base as determined from cloud-layer diagnostic models (Johnson 1978, 1980; Nitta, 1978). These diagnostic studies have shown that environmental subsidence, i.e., subsidence surrounding convective elements, near the level of cloud base, ~960 mb in the GATE region, is a maximum during undisturbed conditions and a minimum during disturbed conditions. Since growth of a mixed layer capped by an inversion and stable layer above is controlled (apart from radiative effects) primarily by a balance between subsidence and buoyancy flux at the inversion level (often related to the surface buoyancy flux), the above diagnostic model results would suggest that, other things being equal, the mixed layers *in regions away from convective systems* should be relatively shallow during undisturbed conditions and deep during disturbed conditions. Evidence from observational studies (e.g., Esbensen, 1975; Payne, 1978[1]; Jalickee and Ropelewski, 1979) suggests that just the opposite is true. However, these and other studies have not isolated and documented the variation of the mixed layer across a tropical wave disturbance *in regions away from the convective systems and their wakes*. This study is an effort to clarify the observations relevant to this matter and to resolve the question raised by the results of these diagnostic studies.

The consistency between diagnostic model results for the cloud-layer and observed mixed-layer structures was earlier examined by Sarachik (1974). He noted that the vertical mass flux in the environment surrounding active convective elements should be consistent with the observed mixed-layer depths in those regions based on relationships derived from simple mixed-layer theory (e.g., Lilly, 1968; Betts, 1973; Tennekes, 1973). Using observations and the diagnostic study of Nitta (1975) for the Barbados Oceanographic and Meteorological Experiment (BOMEX), Sarachik determined that the subsidence diagnosed by Nitta in the cloud environment during undisturbed conditions was too large (by a factor of 2) when compared with simple mixed-layer model predictions. Later work shed light on this discrepancy by showing that the neglect of in-cloud downdrafts in diagnostic models leads to predictions of excessive subsidence in the between-cloud environment (Johnson, 1976; Cho, 1977; Nitta, 1977). Further, Betts (1975) noted that the mixed-layer model should include a term involving detrainment of heat at cloud base when applied to the undisturbed trades where a field of shallow cumulus convection exists.

The questions regarding the large-scale control of the structure and properties of the mixed layer are addressed by introducing a simple model to permit a prediction of the mixed-layer depth and inversion strength in the regions between convective systems. In a simplified way, the convergence into this region of air modified by precipitation downdrafts is taken into account. In this sense the mixed-layer and cloud-layer diagnostic models are coupled; however, cloud base in the cloud-layer model is prescribed as the lifting condensation level of the surface air. Effects of radiative jumps at the top of the unsaturated convectively mixed layer are included, but are clearly of second-order importance in the model proposed here (unlike stratocumulus-topped mixed layers).

[1] Payne, S., 1978: The large-scale structure and properties of the disturbance of 15 to 18 September, 1974, over the GATE B-scale ship array. M.S. thesis, University of Washington, 112 pp.

2. A conceptual model and relevant observations

a. Schematic model: definition of wakes

In order to establish a proper perspective for subsequent discussion, a schematic showing a highly simplified view of the boundary layer in the vicinity of the commonly occurring (Leary and Houze, 1979) GATE mesoscale precipitation systems is introduced at this point in Fig. 1. Specifics of the model will be discussed later. The convective mass flux in updrafts and downdrafts (M_U and M_D) consists of both convective-scale and mesoscale components (Zipser, 1977). Numerous studies have shown that there usually exists a gradual transition from a very shallow wake or density current near the active downdrafts of convective systems to a nearly fully-restored tropical boundary layer well to their rear. This zone of transition may extend over ~100–1000 km in the more intense tropical squall lines (Houze, 1977; Zipser, 1977). In most studies the region of downdraft-modified air and the recovery zone are generally referred to as the wake region. The wake may extend over an area considerably greater than the area of the active convective clouds (Zipser, 1977).

In this study the definition of wake is slightly modified to conform with the zero-order discontinuity model developed in Section 3. In particular, the zone of transition between the heavy rain area near the core of the convective system and the undisturbed region far to the rear is to be modeled as an infinitesimal boundary, across which the thermodynamic fields are discontinuous. The region containing the precipitation is called the *wake* and that outside it is labeled $\bar{A}$ (Fig. 1). In $\bar{A}$ the boundary layer air is assumed horizontally uniform and well mixed with a uniform mixed-layer depth. The mixed layer may be topped by scattered shallow cumulus clouds. Air in this region "outside wakes" is influenced by outflow from precipitation downdrafts; however, when viewed on large space and time scales, it is considered that individual cloud systems within the wake region can be treated in terms of their averaged effects on the boundary layer in $\bar{A}$. A similar philosophy has been adopted in models for the cloud layer, where large-scale space and time averages have been considered (Arakawa and Schubert, 1974). As in Arakawa and Schubert, while variables on the scale of $\bar{A}$ (say, the grid scale in a general circulation model) are assumed horizontally homogeneous, they do vary horizontally on the synoptic scale.

The determination of the position of the boundary between wakes and $\bar{A}$ or, alternatively, the fractional area covered by wakes, is influenced by two considerations. First, for the application of the zero-order discontinuity model to an extensive continuous zone of transition, the boundary should be placed somewhere near the middle of this zone. Second, since a zero-order jump mixed-layer model will be used in $\bar{A}$ and the vertical velocity $\bar{w}$ in the cumulus environment (Fig. 1) to be used with it must be obtained from a cloud-layer diagnostic model (Johnson, 1980), the cumulus environment in $\bar{A}$ should approximately correspond to the cloud environment area in that diagnostic model. Since wake areas normally are greater than the convective draft areas, however, the area to which $\bar{w}$ applies will normally include $\bar{A}$ and portions of wakes external to the deep convective drafts. Unfortunately, since the cloud models used in Johnson (1980) are highly simplified (by necessity), a reasonable estimate of the cloud environment area from it cannot be made. Therefore, the latter consideration does not help much in defining the fractional wake area.

As it turns out, the model results to be reported later are not particularly sensitive to the precise choices of wake areas. Nevertheless, a reasonable definition must be made. Gaynor and Ropelewski (1979) report an average mixed-layer depth of wakes during Phase III of 250 m. We will define as wakes in this study those regions where a modified downdraft–boundary layer air has a mixed-layer depth $\leq$ 300 m. Some of the observations reported in Section 2b used to determine average wake areas have been grouped according to this definition.

b. Mixed-layer observations

In this study we are primarily interested in large-scale boundary layer properties and their behavior in response to the passage of large-scale tropical disturbances. We have used data from a composite of large-scale African wave disturbances (Thompson *et al.*, 1979) in our analysis. In their work, Thompson *et al.* have prepared a composite of six wave disturbances that traversed the GATE A/B, B-scale array during the period 30 August–18 September, 1974 (Phase III). The average wavelength and wave period were 2500 km and 3.5 days, respectively. Rawinsonde observations from A/B, B-scale ships were fitted quadratically in space and linearly over 12 h time intervals by the method of least squares. The data were then composited into eight categories based on the phases of the waves at 700 mb (near the level of maximum wave amplitude). The following notation will be used: 8 refers to the wave ridge, 4 the trough, 2 the position of maximum northerly wind at 700 mb and 6 the position of maximum southerly wind at 700 mb. Categories 1, 3, 5, and 7 occupy intermediate position. In Fig. 2 the virtual static energy $s_v = s(1 + 0.61q)$, where $s = c_pT + gz$ is the dry static energy and q the specific humidity, is presented in the lower

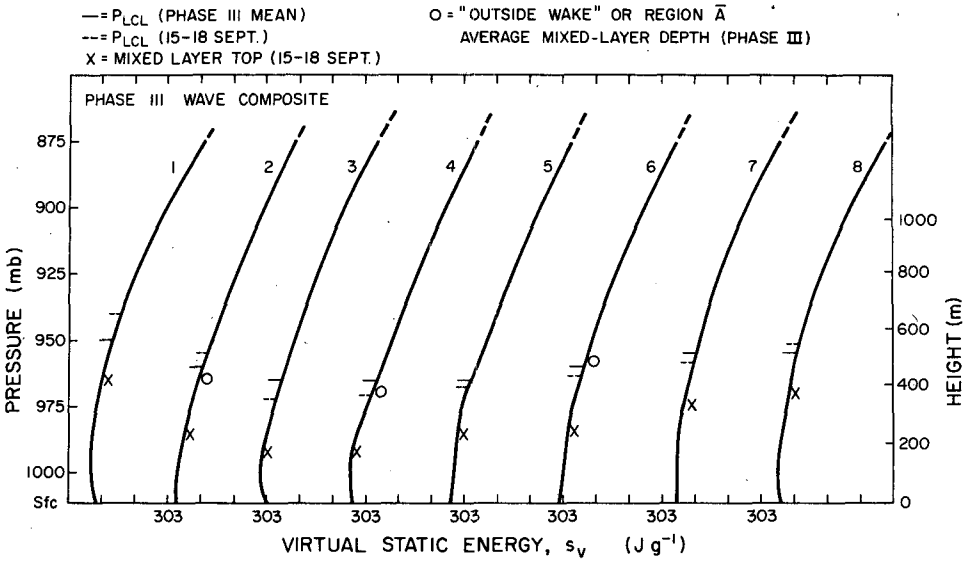

FIG. 2. Atmospheric boundary-layer structure for Thompson *et al.* (1979) composite wave (category 4 = wave trough, category 8 = wave ridge). Data for 15–18 September are for a single wave (from Payne, 1978[1]). P_{LCL} refers to lifting condensation level of air at 1000 mb. Divisions on abscissa represent 1 J g^{-1}. Time and space scales associated with a single category are ~11 h and ~300 km, respectively.

troposphere for the Phase III composite wave.[2] The vertical resolution of the Thompson *et al.* data is 25 mb, except for the 1000–1011 mb layer nearest the surface. Also shown in Fig. 2 are the average heights of the top of the mixed layer determined by Payne (1978)[1] using soundings with 5 mb vertical resolution from the eight B-scale ships for one of the six waves (15–18 September). These soundings, taken at fixed times, are randomly distributed in space relative to the mesoscale convective systems that propagate through the ship array. Payne's results indicate a suppression of the mixed layer that occurs in the region of the wave trough, where precipitation is a maximum. Although statistical information for the ~25 soundings per category was not provided, it is probably true that the minimum average mixed-layer depth in the wave trough region can be attributed to the increased sampling by soundings of mesoscale "wakes" in that region (Zipser, 1977; Gaynor and Ropelewski, 1979). The profiles of s_v in Fig. 2 for all of Phase III from Thompson *et al.* (1979) do not show clear indications of mixed-layer structures because they averaged data without a prior scaling according to mixed-layer depth. In some categories, however, the subjective analysis of the Phase III data suggests mixed layer depths in approximate agreement with those reported for the single 15–18 September wave.

Further analysis of the B-scale sounding data (from World Data Center A, Asheville, NC) for all of Phase III has been carried out to support the model development that follows. Soundings in categories 2, 4 and 6 have been screened to determine what fraction have a well-mixed layer structure and are outside of wakes, i.e., by our earlier definition, have mixed-layer depths > 300 m. The screening was limited to those soundings for which coincident radar data were available in the atlas of Arkell and Hudlow (1977).[3] The radar data were used to determine whether or not precipitation was falling in the immediate vicinity of the sounding at release time. Out of 46, 31 and 35 B-scale soundings in categories 2, 4 and 6, respectively, that were identified as having well-mixed layers with depths > 300 m, all but ~5% were taken in an environment having less than 10% areal coverage of precipitation echoes within a 50 km radius of the station. The average mixed-layer depths for these soundings were 410 ± 108 m, 382 ± 96 m and 484 ± 157 m for categories 2, 4 and 6 respectively. These values, taken as representative of the outside-wake (region $\bar{A}$) mixed-layer depths, are plotted in Fig. 2. The average surface temperatures for these soundings are 26.4 ± 1.0°C, 25.9 ± 1.0°C and 26.1 ± 0.6°C corresponding to categories 2, 4 and 6, respectively. These temperatures are comparable to the *average*

[2] This definition of s_v is equivalent to $s_v = c_p T_v + gz$, where T_v is the virtual temperature, within 0.07% in the lowest 1 km of the atmosphere.

[3] Arkell, R., and M. Hudlow, 1977: *GATE International Meteorological Radar Atlas*. CEDDA, National Oceanic and Atmospheric Administration, 222 pp.

temperature for the wave ridge (category 8) of 26.2°C (Thompson *et al.*, 1979) and are considerably greater than the trough (category 4) average, 25.1°C. Approximately 15% of the soundings in category 4 show mixed-layer depths > 450 m. These findings indicate that even in the convectively-active trough portion of the waves there are regions having mixed layers characteristic of those in the undisturbed wave ridge.

If the fractional numbers of soundings in regions are equated to corresponding fractional areas, estimates of fractional wake areas can be made. However, these estimates will represent upper bounds to the wake areas since a number of soundings that do not exhibit a well mixed structure, for one or more of several possible reasons, may still lie in region $\bar{A}$. The upper bound estimate on fractional areas covered by wakes (as they are defined in this study) for categories 2, 4 and 6 are 50, 70 and 55%, respectively. The observations reported here will later be used as a guide in specifying wake areas in application of the model developed in the next section.

Also indicated in Fig. 2 is the lifting condensation level (LCL) of the air at 1000 mb in each category from both the study of Payne (1978)[1] and Thompson *et al.* (1979). The category-averaged values for the single wave and Phase III composite are in reasonably good agreement. Observations from Fig. 2 are presented primarily to provide a descriptive framework for the model to follow. However, some quantitative information will be taken from Fig. 2: 1) the LCL for assigning cloud base in the cloud-layer model, 2) the lapse rate of s_v above the mixed layer and 3) an estimate of the average depth of spreading downdraft air (Section 5).

Observations for the ridge, where little to no deep convection exists, should be suitable for the application of mixed-layer theory developed for widely scattered cumulus conditions (e.g., Esbensen, 1975; Betts, 1976b; Johnson, 1977). These situations, in the context of the large-scale model to be developed here, can be considered a special case where precipitation downdraft effects vanish.

3. Mixed-layer model

As discussed earlier, the boundary-layer outside wakes ($\bar{A}$ in Fig. 1) is assumed horizontally uniform and well mixed with a uniform mixed-layer depth. It is also assumed that the average vertical velocity $\bar{w}$ corresponds to that determined for the cloud environment region in the cloud-layer diagnostic model of Johnson (1980).

The vertical variation of s_v in $\bar{A}$ is illustrated in Fig. 1 where z_b is cloud base, z_i the mixed-layer top, z_s the base of the mixed layer (very close to the ocean surface) and $\bar{\gamma}_v = ds_v/dz$ is the lapse rate above the mixed layer. The model to be developed here is patterned after the extensively used jump model (Lilly, 1968; Betts, 1973; Carson, 1973; Tennekes, 1973; Deardorff, 1974; Zeman and Tennekes, 1977) modified to include effects of a field of widely scattered shallow cumuli (Betts, 1976b; Johnson, 1977). It is felt that a more complex model designed to take into account the effects of a more realistic capping inversion structure (Betts, 1974; Deardorff, 1979) is not warranted at this preliminary stage in the evaluation of the large-scale response of the boundary layer to deep convection.

Since there is no condensation or evaporation below z_i in $\bar{A}$, the budget for s_v there is (applying the Boussinesq approximation)

$$\frac{\partial s_v}{\partial t} + \nabla\cdot s_v\mathbf{v} + \frac{\partial}{\partial z} s_v w = -\frac{\partial F_R}{\rho\partial z}, \qquad (1)$$

where F_R is the net upward radiative flux, ρ is air density and $\mathbf{v}$ is the horizontal velocity. Integration of (1) over the volume V occupied by $\bar{A}$ between z_s and z_i (not across the jump in s_v from z_i to z_b), designating horizontal averages over this area by an overbar yields

$$\frac{\partial \bar{s}_v}{\partial t} + (\bar{s}_v - \hat{s}_v)\frac{1}{\bar{A}}\frac{d\bar{A}}{dt} + \frac{1}{V}\iiint_V \nabla\cdot s_v\mathbf{v}dV + \frac{\bar{s}_v(\bar{w}_i - \bar{w}_s)}{\Delta z} = \frac{\bar{F}_s - \bar{F}_i + F_{Rs} - F_{Ri}}{\rho\Delta z}, \qquad (2)$$

where subscripts s and i refer to values at z_s and z_i, respectively, $\bar{F}$ is the virtual static energy flux $\rho(\overline{s_v'w'})$, $\Delta z = z_i - z_s$ and

$$\hat{s}_v = \begin{cases} \bar{s}_v & \text{if } d\bar{A}/dt < 0 \\ s_{vd} & \text{if } d\bar{A}/dt > 0. \end{cases}$$

The term involving $\hat{s}_v$ comes from application of Leibniz's rule to the derivative of an integral over the time-varying domain $\bar{A}$. Note that this term is nonzero only when the area $\bar{A}$ is expanding. Air outside $\bar{A}$ is assumed to have uniform properties characteristic of downdraft wakes, i.e., a vertically constant virtual static energy s_{vd}. Since z_s is very close to the ocean surface, we will set $z_s = 0$ so that $\Delta z = z_i$ and $\bar{w}_s = 0$.

Using the divergence theorem and noting that $\hat{k}\cdot\mathbf{v} = 0$ (refer to Fig. 3), the third term in (2) becomes

$$\iiint_V \nabla\cdot s_v\mathbf{v}dV = \iint_S \hat{n}\cdot s_v\mathbf{v}dS = \iint_{S_{in}} \hat{n}\cdot s_{vin}\mathbf{v}_{in}dS_{in} + \iint_{S_{ou}} \hat{n}s_{vou}\mathbf{v}_{ou}dS_{ou}, \qquad (3)$$

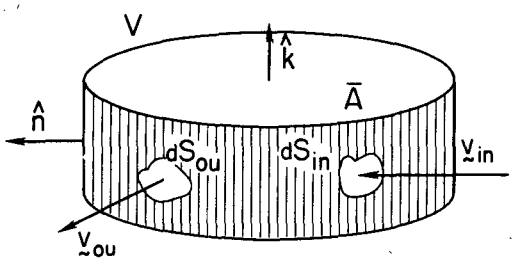

FIG. 3. Volume V occupied by region $\bar{A}$ outside wakes. dS is an increment of area on the side of the volume and $\hat{n}$, $\hat{k}$ are local horizontal, vertical unit vectors, respectively. Other symbols are defined in the text.

where the subscripts *in*, *ou* refer to air moving in and out of V, respectively. Since air within V is well mixed, $s_{vou} = \bar{s}_v =$ constant. Air flowing into V will be associated with convective-scale and mesoscale downdrafts, i.e., $s_{vin} = s_{vd}$. Zipser (1977) contends that the greatest fraction of the wake air is from convective-scale downdrafts. The precise relation of s_{vin} to the thermodynamic properties of downdrafts, however, is not well-known, particularly considering the modification of downdraft air by sensible and latent heat fluxes from the ocean surface. Owing to the additional uncertainty in determining s_v in modeled downdrafts, for example, specification of level of origin of downdraft, etc., a budget analysis to determine s_{vin}, though possible, is not carried out. In application of the model here, GATE observations of s_{vin} will be used. With $s_{vin} = s_{vd}$ = constant, (3) becomes

$$\iiint_V \nabla\cdot s_v\mathbf{v}dV = s_{vd}\iint_{S_{in}} \hat{n}\cdot\mathbf{v}_{in}dS_{in} + \bar{s}_v\iint_{S_{ou}} \hat{n}\cdot\mathbf{v}_{ou}dS_{ou}. \quad (4)$$

Integration of the mass continuity equation yields

$$\frac{1}{V}\iiint_V \nabla\cdot\mathbf{v}dV = -\frac{\bar{w}_i}{z_i} = \frac{1}{V}\left[\iint_{S_{in}} \hat{n}\cdot\mathbf{v}_{in}dS_{in} + \iint_{S_{ou}} \hat{n}\cdot\mathbf{v}_{ou}dS_{ou}\right]. \quad (5)$$

Combining (2), (4) and (5), we get

$$\frac{\partial\bar{s}_v}{\partial t} = \frac{\bar{F}_s - \bar{F}_i + F_{Rs} - F_{Ri}}{\rho z_i} + (\bar{s}_v - s_{vd})\frac{1}{V}\times\iint_{S_{in}} \hat{n}\cdot\mathbf{v}_{in}dS_{in} - (\bar{s}_v - \hat{s}_v)\frac{1}{\bar{A}}\frac{d\bar{A}}{dt}. \quad (6)$$

Since $\mathbf{v}_{in}$ is associated with outflow from convective downdrafts,

$$\frac{1}{V}\iint_{S_{in}} \hat{n}\cdot\mathbf{v}_{in}dS_{in} = \frac{\Delta M_D}{\rho\Delta z} \approx \frac{M_{Db}}{\rho z_i},$$

where $\Delta M_D = M_D(z_i) - M_D(z_s)$, M_D is the cumulus plus mesoscale downdraft mass flux and $M_{Db} \equiv M_D(z_b)$. Thus, we can write (6) as

$$\frac{\partial\bar{s}_v}{\partial t} = \frac{\bar{F}_s - \bar{F}_i + F_{Rs} - F_{Ri}}{\rho z_i} - D - (\bar{s}_v - \hat{s}_v)\frac{1}{\bar{A}}\frac{d\bar{A}}{dt}, \quad (7)$$

where

$$D = \frac{M_{Db}}{\rho z_i}(s_{vd} - \bar{s}_v).$$

The term D represents the effects of downdraft outflow of cool air and acts to reduce $\bar{s}_v$ since M_{Db} and $s_{vd} - \bar{s}_v$ are both <0. The last term contributes only when the area $\bar{A}$ is increasing ($d\bar{A}/dt > 0$) and has the effect of reducing $\bar{s}_v$ as the expanding region occupies areas of cooler downdraft air.

The budget for s_v at cloud base z_b in region $\bar{A}$ is where only shallow cumuli exist is that presented in Betts (1976b) and Johnson (1977):

$$\frac{\partial\bar{s}_{vb}}{\partial t} + \left(\bar{w}_b - \frac{dz_b}{dt}\right)\bar{\gamma}_v = -\delta_b\Delta_i + Q_{Rb}, \quad (8)$$

where subscript b denotes values at z_b, a tilde represents an average over the cumulus environment, δ_b is the total detrainment rate for all clouds at z_b, Δ_i is the inversion strength $\bar{s}_v(z_b) - \bar{s}_v$, and Q_{Rb} is the net radiative heating rate at z_b. In (8) it has been assumed that all updrafts carry air with average mixed layer properties (see Johnson (1977) for some justification) and that the liquid water content at cloud base in cumulus updrafts is vanishingly small. Further, it is assumed that shallow cumulus downdrafts do not affect the budget at z_b. This assumption is consistent with Betts' (1973) argument that cloud parcels in nonprecipitating clouds, following ascent to cloud top, will not descend all the way back to cloud base because of dilution or mixing with the environment during ascent. Although $\bar{F}_i$ includes contributions from both turbulent eddies and cumulus updrafts and downdrafts (Esbensen, 1975), these assumptions also allow us to approximate $\bar{F}_i$ in (7) by $\bar{F}_i$ (Johnson, 1977). Subtraction of (7) from (8) then gives an expression for the inversion strength Δ_i

$$\frac{\partial\Delta_i}{\partial t} + \left(\bar{w}_b - \frac{dz_b}{dt}\right)\bar{\gamma}_v = \frac{\bar{F}_i - \bar{F}_s}{\rho z_i} - \delta_b\Delta_i + \Delta Q_R + D + (\bar{s}_v - \hat{s}_v)\frac{1}{\bar{A}}\frac{d\bar{A}}{dt}, \quad (9)$$

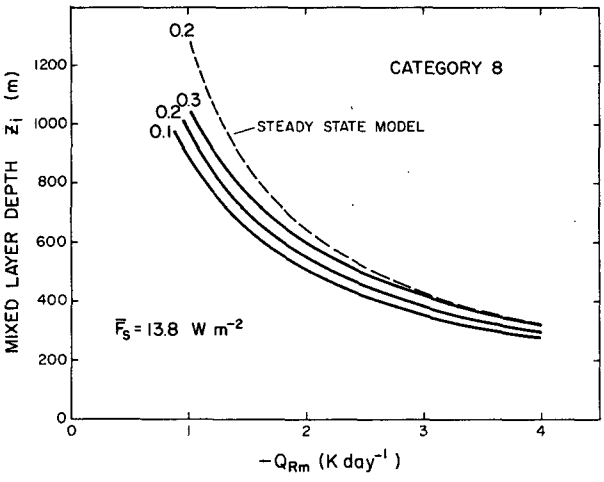

FIG. 4. Mixed-layer depth z_i versus average mixed-layer net radiative heating rate Q_{Rm} for wave ridge. Values of k are indicated at ends of curves.

where $\Delta Q_R = Q_{Rb} - Q_{Rm}$ is the jump in the radiative heating rate at the inversion, Q_{Rm} being $(F_{Rs} - F_{Ri})/\rho z_i$, the average radiative heating rate in the mixed layer.

An expression for the time variation of z_i is obtained by integrating (1) from z_i to z_b in the cumulus environment and then letting $z_b - z_i \to 0$ (Lilly, 1968):

$$\frac{dz_i}{dt} - \tilde{w}_i = -\frac{\bar{F}_i}{\rho\Delta_i} + \frac{F_{Rb} - F_{Ri}}{\rho\Delta_i}. \tag{10}$$

Transports due to noncloud turbulent eddies vanish at z_b, i.e., in (10) $\bar{F}_b = 0$. Defining the jump in the radiative flux across the inversion as $\Delta F_R = F_{Rb} - F_{Ri}$ and using (10) in (9) with $\tilde{w}_b = \tilde{w}_i$ we have

$$\frac{\partial\Delta_i}{\partial t} = \frac{\Delta F_R - \bar{F}_i}{\rho\Delta_i}\bar{\gamma}_v + \frac{\bar{F}_i - \bar{F}_s}{\rho z_i} - \delta_b\Delta_i + \Delta Q_R + D + (\bar{s}_v - \hat{s}_v)\frac{1}{\bar{A}}\frac{d\bar{A}}{dt},$$

$$\frac{\partial z_i}{\partial t} = -\mathbf{v}\cdot\nabla z_i + \tilde{w}_i + \frac{\Delta F_R - \bar{F}_i}{\rho\Delta_i}. \tag{11}$$

The term involving the advection of z_i is present because, although assumed horizontally homogeneous in $\bar{A}$, z_i does vary on the much larger wave scale. The set (11) can be solved to give the time variation of Δ_i, z_i when coupled with a cloud-layer diagnostic model (Betts, 1976b; Johnson, 1976; Nitta, 1977) that will provide the time variation of δ_b, D and $\tilde{w}_i$. Large-scale thermodynamic observations give $\bar{\gamma}_v(t)$. A determination of the radiative jumps at the inversion must also be made. Although previous studies of the dry convective boundary layer have usually neglected these jumps, Manton (1978) has suggested they may be important. Estimates of ΔQ_R, ΔF_R are made in the next section based on application of (11) to undisturbed conditions.

Finally, some closure assumption is needed. As in Esbensen (1975) and Johnson (1977), we set

$$\bar{F}_i = -k\bar{F}_s, \tag{12}$$

where k is a constant. Though proper treatment of the turbulent kinetic energy budget within the inversion suggests k to be a function of the inversion strength itself (Zilitinkevich, 1975), a simple constant k is used here. Betts (1976b) notes that the theoretical validity of (12) for the case of cumulus-topped mixed layers in not clear; however, if the cloud coverage is small, ~10% or less, then its use is probably tolerable. A question also has to be raised regarding this type of closure if there exists a significant vertical gradient of radiative heating rate in the boundary layer, possibly contributing to the generation of turbulent kinetic energy in the mixed layer and/or inversion above (Manton, 1978). This process should be especially important for stratocumulus-topped mixed layers (Deardorff and Businger, 1980). For the relatively weak inversions reported in GATE, this effect is felt to be minimal, and in the context of the model used here will be considered as contributing to a slight adjustment in k. Nicholls and LeMone (1980) have reported $k \approx 0.2$ for the GATE fair weather boundary layer with an approximate 10% coverage of shallow cumuli. Results of some sensitivity tests to the choice for k will be shown.

4. Estimates of radiative heating effects

A determination of some of the effects of radiative heating is possible from a study of the undisturbed boundary layer (e.g., Betts, 1975; Esbensen, 1978). When no precipitation downdrafts exist, (7) using (12) becomes

$$\frac{\partial\bar{s}_v}{\partial t} = (1 + k)\frac{\bar{F}_s}{\rho z_i} + Q_{Rm}. \tag{13}$$

For the steady-state mixed layer the flux convergence of heat from the ocean surface and stable layer above is balanced by an average net radiative cooling in the mixed layer ($Q_{Rm} < 0$). The data of Thompson *et al.* indicate that the wave ridge (category 8) is nearly in steady-state, with $\partial\bar{s}_v/\partial t = +0.3$ K day^{-1}. The observed precipitation for category 8 is quite small, 4 mm day^{-1}.

If (13) is applied to data for category 8 where $\bar{F}_s = 13.8$ W m^{-2}, then solutions for z_i, Q_{Rm} shown in Fig. 4 are obtained. Reported mixed-layer depths for undisturbed conditions in GATE range from 400 to 500 m (Brümmer, 1978; Gaynor and Ropelewski,

TABLE 1. Radiative flux jump ΔF_R at inversion. Units: W m^{-2}.

Q_{Rb} (K day^{-1})	−1	−2	−3
$k = 0.1$	+8.4	+7.0	+5.6
$k = 0.2$	+4.6	+3.2	+1.8
$k = 0.3$	+0.7	−0.6	−2.0

1979; Payne, 1978[1]). From Fig. 4 it is seen that these values of z_i correspond to a Q_{Rm} of −2 to −3 K day^{-1}. Based on six-hourly radiative heating estimates from Cox and Griffith (1979), a Q_{Rm} for category 8 of about −2 K day^{-1} is obtained (Johnson, 1980). Had Cox and Griffith used in their calculations vertical temperature and moisture distributions containing the detailed structure of GATE mixed layers with capping stable layers, rather than smoothed vertical profiles, larger cooling rates would have been diagnosed (Manton, 1978). A general study of radiative heating rates for the GATE boundary layer, including the cooling-enhancement effect of the water dimer (Stephens, 1976; Burroughs, 1979), is probably needed. The dashed curve in Fig. 4 indicates that a steady-state model for the mixed layer in category 8 agrees fairly well with one in which the time variation of s_v is included.

In most studies of the mixed layer with no clouds or widely scattered cumuli above, ΔQ_R and ΔF_R have been neglected. We now try to determine their values based on a steady-state model. For this case (8) becomes

$$\tilde{w}_b\tilde{\gamma}_v = -\delta_b\Delta_i + Q_{Rb}. \tag{14}$$

Combining (14) with (10) for the steady-state case we have

$$\tilde{w}_b\tilde{\gamma}_v = \delta_b(\Delta F_R - \tilde{F}_i)/\rho\tilde{w}_b + Q_{Rb}$$

or with (12)

$$\Delta F_R = \rho\delta_b^{-1}[\tilde{\gamma}_v\tilde{w}_b^2 - Q_{Rb}\tilde{w}_b] - k\tilde{F}_s. \tag{15}$$

Eq. (15) may be solved for ΔF_R using data for category 8, but the results must clearly be viewed with caution considering the simplicity and approximations of the model. With $\delta_b = 7.7 \times 10^{-5}$ s^{-1}, $\tilde{w}_b = -2.3$ cm s^{-1} and $\tilde{\gamma}_v = 1.8$ J kg^{-1} m^{-1} for category 8 (Johnson, 1980), ΔF_R as a function of k and Q_{Rb} is computed and shown in Table 1. A value of ΔF_R of +3.2 W m^{-2} corresponds to an average Q_R of −2.5 K day^{-1} in a transition layer 100 m deep. Negative values of ΔF_R are not physically reasonable since they would imply a net radiative heating in the transition layer, opposite to what one would expect for a sharp decrease in specific humidity with height.

Combining the results shown in Table 1 with those from Fig. 4, assuming an average undisturbed mixed-layer depth of 450 m, $\Delta Q_R = Q_{Rb} - Q_{Rm}$ is computed (Table 2). Manton (1978) has shown using hypothetical data for a 500 m deep mixed layer capped by an extremely dry inversion that $\Delta Q_R > 0$. G. Stephens has kindly carried out clear-sky radiative calculations using the model of Stephens (1976) applied to the GATE undisturbed mixed layer structure reported by Gaynor and Ropelewski (1979). His results indicate that $\Delta Q_R \sim 0.5$ K day^{-1} (corresponding to $k = 0.2$, $Q_{Rb} = -2$ K day^{-1} in Table 2).

Based on the above results $\Delta Q_R = +0.5$ K day^{-1} and $\Delta F_R = +3.2$ W m^{-2} are used in subsequent application of the model. These values, determined for undisturbed conditions, are also applied, for simplicity, to the wave-trough region, since determination of ΔF_R, ΔQ_R in that very cloudy region (Johnson, 1980) is extremely complicated. Comparative runs for $\Delta F_R = 0$ and $\Delta Q_R = 0$ will be shown in Section 6. Fortunately, for the purposes of this paper, $z_i(t)$ determined from (11) is not particularly sensitive to the choices of ΔF_R, ΔQ_R. The inversion strength, however, is rather sensitive to ΔF_R, since (for steady-state conditions)

$$\Delta_i = \frac{k\tilde{F}_s + \Delta F_R}{-\rho\tilde{w}_b}. \tag{16}$$

For category 8, $k = 0.2$, $\Delta_i = 0.12$ K for $\Delta F_R = 0$, whereas $\Delta_i = 0.26$ K for $\Delta F_R = +3.2$ W m^{-2} (here Δ_i is converted to units of K using $c_p = 1.004$ kJ kg^{-1} K^{-1}).

5. Determination of model variables

a. Surface buoyancy flux $\tilde{F}_s$

Values of sensible and latent heat flux reported by Thompson *et al.* (1979) may be appropriate to use for determining the surface buoyancy flux in the region outside wakes ($\tilde{F}_s$) in the undisturbed wave-ridge region, but certainly not in the wave trough. The spreading of downdrafts over large areas during disturbed conditions complicates the determination of $\tilde{F}_s$ at those times. For example, Gaynor and Ropelewski (1979) show that the surface sensible heat flux in the wakes of precipitation systems is 2.5 times greater than that during undisturbed

TABLE 2. Radiative heating rate jump ΔQ_R at inversion. Units: K day^{-1}

Q_{Rb} (K day^{-1})	−1	−2	−3
$k = 0.1$	1.3	0.3	−0.7
$k = 0.2$	1.5	0.5	−0.5
$k = 0.3$	1.8	0.8	−0.2

conditions during Phase III of GATE. The latent heat flux, on the other hand, is slightly smaller in wakes due primarily to lighter winds. The two effects combine to give a ratio κ of surface virtual static energy flux in wakes to that in undisturbed conditions of 1.39 for Phase III (Gaynor and Ropelewski).

This estimate of κ may be used to determine $\bar{F}_s$ for each wave category. The total area-averaged surface flux of s_v, defined as $[F_s]$, is

$$[F_s] = \sigma F_{sw} + (1 - \sigma)\bar{F}_s, \tag{17}$$

where σ is the fractional area occupied by downdraft wakes and F_{sw} is the wake area-averaged surface flux of s_v. Assuming $\kappa = F_{sw}/\bar{F}_s$ for each category,

$$\bar{F}_s = [F_s]/[1 + (\kappa - 1)\sigma]. \tag{18}$$

The area distribution of wakes in each category is suggested from the observational results of Section 2; however, the fractional area amounts given were only upper-bound estimates. We choose to relate the category distribution of σ both to the observed estimates for categories 2, 4 and 6 stated earlier and to the distribution of precipitation across the wave (Thompson *et al.*, 1979), maintaining an average area coverage by wakes for the entire wave of ~30% (Gaynor and Ropelewski, 1979). Accordingly, we specify for categories 1–8, σ = 0.10, 0.30, 0.50, 0.60, 0.50, 0.30, 0.10, 0.05, respectively. $\bar{F}_s$ computed from (18) is shown in Fig. 5. As expected, values in regions between precipitating clouds are less than the area-averaged values (from Thompson *et al.*, 1979). A slight increase in $\bar{F}_s$ is seen in the wave-trough region due to the presence of somewhat cooler air there.

b. Cloud-layer terms

The total area-averaged stability $[\gamma_v]$ of the air above the mixed-layer derived from Fig. 2 is shown in Fig. 5 for the composite wave. $\bar{\gamma}_v$ appropriate for region $\bar{A}$ in Fig. 1 cannot be determined from the data of Thompson *et al.*; however, it is not expected that $\bar{\gamma}_v$ should be significantly different from $[\gamma_v]$, especially since rawinsonde ballon releases were often timed to avoid precipitating systems (Frank, 1979). It is seen from Fig. 5 that the lower troposphere, as expected, is more stable in the wave-trough region than in the ridge.

Environmental subsidence at cloud base $\tilde{w}_b$ (subsidence in the region surrounding active clouds) is shown in Fig. 5 as computed in Johnson (1980). This subsidence, as noted in Fig. 1, applies to area $\bar{A}$ as well as the portions of wakes away from deep convective drafts. It is not possible with the cloud layer diagnostic model to determine anything other than a horizontally uniform $\tilde{w}$. It may be that $\tilde{w}$ over $\bar{A}$ is, in actuality, slightly different than that over the wake area outside of the convective drafts, but there does not seem to be a physical basis nor observations to determine what difference might exist. In this simplified model $\tilde{w}_b$ diagnosed by the cloud model is assumed to apply to the area $\bar{A}$. When cumulus and mesoscale downdrafts are neglected, strong subsidence is diagnosed in the wave trough (categories 4, 5). When included, there is a minimum in the diagnosed $\tilde{w}_b$ at and in advance of the wave trough. Mixed-layer model predictions will be made for both $\tilde{w}_b$ profiles. Nitta (1978), using a diagnostic model quite different from that of Johnson (1980), obtained a distribution of $\tilde{w}_b$ across a GATE composite wave that is quali-

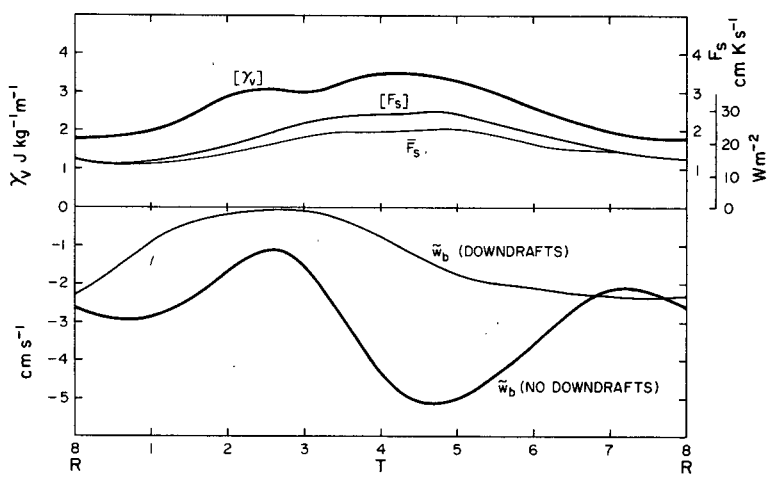

FIG. 5. Lapse rate above mixed layer $[\gamma_v]$, surface buoyancy flux (total area-averaged value, $[F_s]$, and average over $\bar{A}$, $\bar{F}_s$) and vertical velocity in the cloud environment at cloud base (with and without downdrafts) for composite wave. R = ridge and T = trough.

tatively the same as that shown in Fig. 5 for the downdraft case.

The mass detrainment rate by cumulus clouds δ_b (Fig. 6) is a minimum at and in advance of the wave trough, and a relatively constant maximum in the wave ridge. The former feature is associated with reduced shallow cumulus activity in the wave trough (Johnson, 1978; Nitta, 1978), probably in response to stabilization of the subcloud layer by convective downdrafts. Shallow cumuli are prevalent in the ridge and the term containing δ_b in the heat budget at z_b is important there (see also Betts, 1976b).

c. Downdraft detrainment

As noted earlier, determination of $D = M_{Db}(s_{vd} - \bar{s}_v)/\rho z_i$ is not straightforward. Downdraft air will enter $\bar{A}$ for two reasons: 1) $\bar{A}$ itself includes the outer portions of wakes, and 2) because long time averages are considered, residual downdraft air may be present in $\bar{A}$ due to previously-existing convection. Since both cumulus and mesoscale downdraft mass fluxes contribute to the spreading of downdraft air, the sum of these two contributions (from Johnson, 1980) is used for M_{Db}. Although formally z_i is the mixed-layer depth in region $\bar{A}$, conceptually in D it should be the depth associated with spreading downdraft air. For this reason we use for z_i in D the mixed-layer depths for the composite wave indicated in Fig. 2 (from Payne, 1978),[1] expecting these values to crudely approximate this appropriate depth. The wave variation of z_i thus determined is consistent with the observed variation in cloud-base level across the wave (Fig. 2).

The total area-averaged s_v for the mixed layer is

$$[s_v] = \sigma s_{vd} + (1 - \sigma)\bar{s}_v$$

or

$$\bar{s}_v - s_{vd} = ([s_v] - s_{vd})/(1 - \sigma). \qquad (19)$$

σ in (19) has been earlier specified in the determination of $\bar{F}_s$. Average downdraft air or wake properties are taken from Gaynor and Ropelewski (1979). Their work gives for Phase III $s_{vd} = 301.4$ J g^{-1} based on observations from the ship *Oceanographer*. We will use this value for s_{vd} and assume, for simplicity, that it is the same for each wave category. Clearly, this assumption is not totally satisfactory, and in a complete model s_{vd} should be calculated explicitly.

Variations in $[s_v]$ from one category to the next are determined from Fig. 2. These observations from Thompson *et al.* represent contributions from the entire GATE B-scale ship array whereas Gaynor and Ropelewski's data are exclusively from the *Oceanographer*. An adjustment is made to the category-average values of s_v in Fig. 2 by subtracting from each value the difference between the Phase III average s_v from Thompson *et al.* and that from Gaynor and Ropelewski (303.2 and 302.6 J g^{-1}, respectively). The latter average is determined by assuming an average 30% area coverage of wakes during Phase III and using the undisturbed and wake thermodynamic profiles from Fig. 5 of Gaynor and Ropelewski. The results (Table 3) indicate that $\bar{s}_v - s_{vd}$ is a minimum in the trough, as might be expected, where the environment is somewhat cooler than in the ridge, due to increased downdraft activity. The composite wave average value of 1.7 J g^{-1} is comparable to the difference in mixed layer s_v between GATE undisturbed and disturbed conditions reported by Brümmer (1978).

The downdraft term D is presented in Fig. 6. A primary maximum is found in the wave trough with a much smaller secondary peak near category 1. These broad features are primarily accounted for by the wave distribution of M_{Db} (Johnson, 1980). The minimum in categories 2 and 3 may not be real, but rather a manifestation of errors in the computed residuals for the cloud layer. This data problem can be seen best by comparing the apparent total heat source (integrated through the depth of the troposphere) derived from large-scale rawinsonde observations, F (computed), with the surface sensible plus latent heat flux, F (observed). The computed F, on which M_{Db} and D are based, is considerably smaller than the observed values in categories 2 and 3. Note that the shape of D closely approximates that of F (computed). Thompson *et al.* (1979) chose to adjust F (computed) through the entire troposphere in such a way that the observed and computed values of F at the surface were identical. Johnson (1980) did not make such an adjustment. When interpreting results, this dis-

TABLE 3. Virtual static energy for total area $[s_v]$, downdraft air s_{vd} and environment–downdraft difference $\bar{s}_v - s_{vd}$. Units J g^{-1}.

	Category								
	1	2	3	4	5	6	7	8	Mean
$[s_v]$	303.2	302.8	302.3	302.0	302.1	302.5	302.9	303.1	302.6
s_{vd}	301.4	301.4	301.4	301.4	301.4	301.4	301.4	301.4	301.4
$\bar{s}_v - s_{vd}$	2.0	2.0	1.8	1.5	1.4	1.6	1.7	1.8	1.7

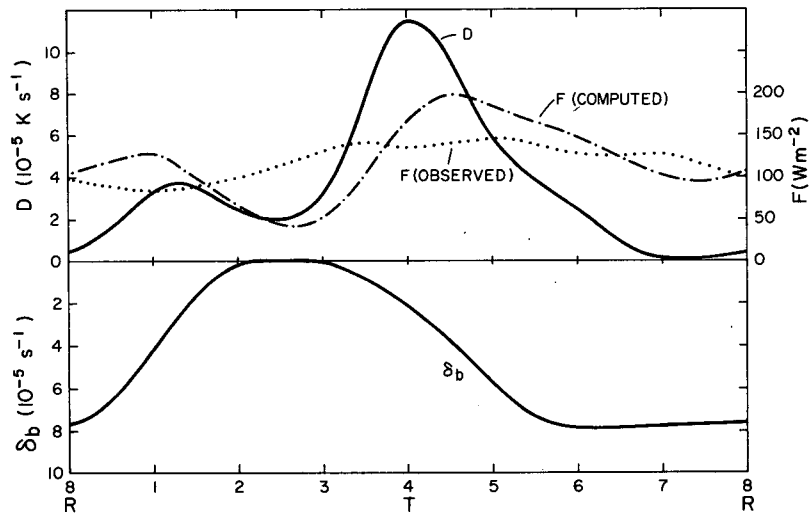

FIG. 6. Downdraft detrainment D, computed and observed surface total heat flux, F and cumulus detrainment rate at cloud base δ_b for composite wave.

crepancy and the possible underestimate of downdraft intensity in categories 2 and 3 should be kept in mind.

d. Horizontal advective effects

The horizontal advective term in (11) cannot be determined directly since information regarding the spatial distribution of z_i over the B-scale ship array is not available. This term is approximated by $u\partial z_i/\partial x \approx u/c\partial z_i/\partial t$ (c = phase speed of westward propagating waves = 8 m s^{-1}), where meridional advection has been neglected. The second equation in (11) then becomes

$$\frac{\partial z_i}{\partial t} = \left(\bar{w}_i + \frac{\Delta F_R - \bar{F}_i}{\rho \Delta i}\right)\Big/(1 + u/c). \qquad (20)$$

Since the flow near the top of the mixed layer in the GATE region is westerly and the waves propagate from east to west, the advection term has the effect of reducing the time rate of change of z_i. Values of u as a function of height and wave category are taken from Thompson *et al.* (1979).

e. Effect of changing area $\bar{A}$

As noted before, the term in (11) involving area change with time is only nonzero when the area is expanding. Since $\sigma = 1 - \bar{A}/A$, where A is the total area, we have for $\sigma < 1$

$$\frac{1}{\bar{A}}\frac{d\bar{A}}{dt} = \frac{1}{(\sigma - 1)}\frac{d\sigma}{dt}.$$

Thus, for $d\bar{A}/dt > 0$,

$$(\bar{s}_v - \hat{s}_v)\frac{1}{\bar{A}}\frac{d\bar{A}}{dt} = (\bar{s}_v - s_{vd})\frac{1}{\sigma - 1}\frac{d\sigma}{dt}.$$

This term is evaluated using Table 3 and σ given in Section 5a.

6. Composite wave results

With terms other than z_i, Δ_i in (11) now specified by wave category and using the closure assumption (12), the set (11) may be solved for $z_i(t)$ and $\Delta_i(t)$ after initial conditions are imposed. The time dependence of the category-averaged variables discussed in Section 5 is established using an average 10.6 h interval between individual categories (Thompson *et al.*, 1979). A linear variation of $\bar{w}_i$ with height is assumed between $z = 0$ and $z = z_b$. Results for $k = 0.2$ are shown since the qualitative findings of this paper are not changed by other choices for k (within reasonable bounds).

Integration is begun in category 8, where conditions are expected to be nearest to steady state, using initial values of z_i, Δ_i appropriate for steady-state conditions (450 m, 0.26 K, respectively). A fourth-order Runge–Kutta scheme is used with a time increment of 1.325 h and (11) is solved for the entire 3.5-day period of the composite wave. Except for an unrealistic case where D has been set to zero, z_i, and Δ_i return closely to their initial values after one wave cycle. This finding suggests that the recovery period of the mixed layer following extensive deep convective activity is short compared to the time scale of the wave.

Computations for four cases are shown in Fig. 7. First consider the case where cloud downdrafts are

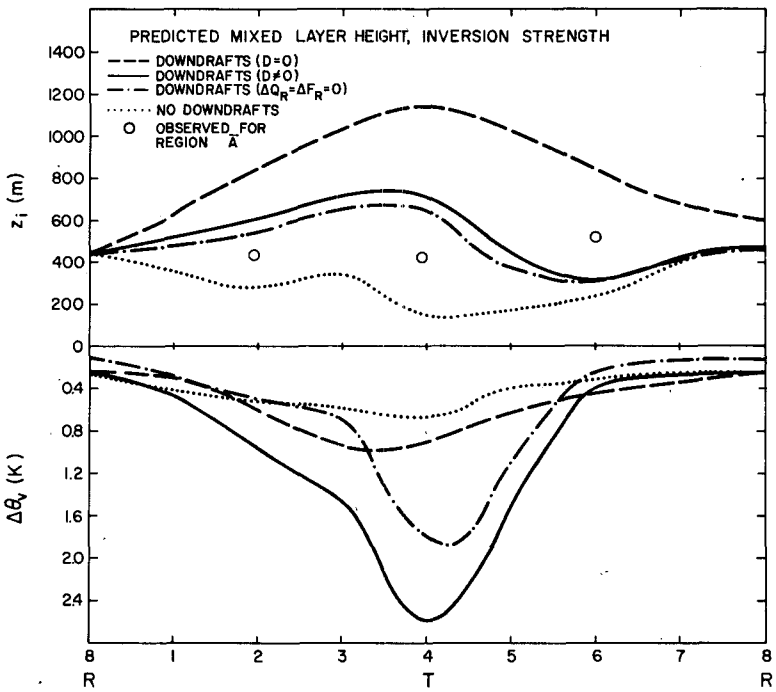

FIG. 7. Predicted mixed-layer depth and inversion strength for composite wave (k = 0.2).

neglected in the cloud-layer diagnostic model. As pointed out earlier (Fig. 5), very strong environmental subsidence $\bar{w}_b$ is then diagnosed in the wave trough. Consequently, the predicted mixed-layer depth in the trough is very shallow, well below the observed estimates for $\bar{A}$ taken from Fig. 2. This result has a possibly important implication for cumulus parameterization theories of the Ooyama (1971) or Arakawa and Schubert (1974) type [on which the diagnostic model of Johnson (1980) is based]. It suggests that the neglect of cloud downdrafts in such schemes may lead to predicted mixed layers that are excessively shallow. One possible response is, after a period of time, a considerably reduced level or even a cut off of further convective activity.

The solution for z_i for the case where cloud downdrafts and the detrainment term D are included gives a more realistic result. Compared to the case discussed above, a relatively constant z_i is predicted across the entire wave. There is an oscillation, however, with a maximum z_i in category 4, which can be attributed to the minimum in D in categories 2 and 3 discussed earlier and the small values of $\bar{w}_b$ in advance of the trough. By looking at the behavior of the inversion strength (expressed in Fig. 7 as $\Delta\theta_v = (\theta/c_pT)\Delta_i$), an explanation for the relatively constant z_i prediction in this case can be found. z_i is kept from increasing to excessively large values in the wave trough in the presence of very weak subsidence because Δ_i increases markedly in the trough [see Eq. (11)]. This increase in the inversion strength is accomplished by the outflow of cool air from downdrafts [term D in (11)]. If D is neglected, Δ_i remains small and z_i becomes unrealistically large, as also shown in Fig. 7. Note that z_i is not particularly sensitive to the radiative jumps ΔQ_R, ΔF_R, although Δ_i is. The effect of the area change term in (11) on the results is small. It is zero before category 4 (where $d\bar{A}/dt < 0$) and reaches a maximum in category 6 where the computed z_i is 10% less with the term included than without.

Since findings of this study are dependent on diagnostic model results for the cloud layer, some discussion of the issue of sensitivity, such as the dependence of z_i on $\bar{w}_b$, has been given. Nitta (1978), applying a different diagnostic model to a similar wave composite for Phase III of GATE, diagnoses nearly identical environmental subsidence in the wave trough, but approximately one-half the subsidence in the wave ridge as found by Johnson (1980). The difference in the results can be attributed to the fact that Nitta's method diagnoses considerable downdrafts within shallow cumulus clouds in the GATE region. It is not obvious, however, that the predicted mixed-layer depth in the ridge will be different using Nitta's

$\bar{w}_b$, since the mass detrainment rate at cloud base δ_b also is different (though not given in his paper). The question of which diagnosed $\bar{w}_b$ is correct in the ridge may not be answerable from application of the mixed-layer model developed here. It should be noted, though, that Johnson (1980) uses another constraint to determine $\bar{w}_b$, namely, that the diagnosed mass and moisture fluxes at cloud base are such that there is a proper balance of the water vapor budget for the subcloud layer.

7. Model and observation limitations

A primary limitation of the mixed-layer model, when viewed in its coupled context with a diagnostic model for the cloud layer, is the inability to accurately determine the average properties of the downdraft outflow air. Ideally, these properties should be determined from a thermodynamic budget in the downdraft region, with a proper consideration of cumulus and mesoscale downdraft transports and sensible and latent heat fluxes from the ocean surface. A fully-coupled model will require a proper treatment of the budget for this region.

A number of assumptions have been made in the development of the model that affect the results described here in a quantitative (though not qualitative) way. Certain of these pertaining to (i) the fractional area covered by wakes in each category, (ii) thermodynamic properties of wakes, (iii) horizontal advective effects and (iv) the depth of spreading downdraft air and (v) subsidence velocity at the top of the mixed layer require further observational verification. These questions need to be addressed in future analysis efforts involving GATE boundary-layer data.

The cloud layer diagnostic models (e.g., Nitta, 1977; Johnson, 1980) used to determine the environmental subsidence at cloud base are themselves not fully-closed models. For example, Nitta (1977) requires a parameterization of the rain process, Johnson (1980) specifies parameters of the convective-scale and mesoscale downdrafts and both assume thermodynamic properties of downdrafts. Further, the convective source terms used to obtain the cloud mass transports are subject to errors, particularly due to uncertainties in net radiative heating rates in the vicinity of clouds. Nevertheless, it is felt that the model results reported in the present study will not be qualitatively changed by improvements or refinements of the cloud-layer models.

8. Discussion and summary

A simple model is proposed to investigate the large-scale response of the mixed layer to the passage of tropical wave disturbances. The mixed layer as defined here refers to that found in regions surrounding precipitating systems where there has been some recovery (~50%, though this value is not precisely determined) toward equilibrium depth following convection. The typically observed zone of transition from shallow wakes near the core of convective systems to an undisturbed mixed layer well to the rear, often extending over ~100 km, is modeled as a zero-order discontinuity. Thus, two distinct areas are defined: the "wake" region and the region "outside wakes", with the latter having a vertical velocity corresponding to that determined for the cloud environment (the region surrounding convective-scale and mesoscale cloud systems) by cloud-layer diagnostic models (e.g., Nitta, 1977; Johnson, 1980). In summary, the horizontal structure of the model is the simplest one can conceive for this problem, namely, a zero-order discontinuity between wakes and the region outside wakes.

The vertical structure is equally simple, essentially an adaptation of the jump model of Lilly (1968). Effects of jumps in the radiative flux and heating rate across the mixed layer inversion are included. The mixed-layer model is coupled with a cloud layer diagnostic model that gives information on the vertical motion field within the cloud layer above.

An observational study of the GATE boundary layer has yielded important information regarding the mixed layer to support the proposed model. In particular, it has been estimated that even in the convectively-active trough portion of the Thompson *et al.* (1979) composite Phase III GATE wave, a considerable fraction ($\leqslant$30%) of the total area has a mixed-layer depth (~380 m) only slightly less than the average (~450 m) of those reported for GATE undisturbed regions by several studies (Brümmer, 1978; Gaynor and Ropelewski, 1979; Payne, 1978[1]). About 15% of the trough area has a mixed-layer depth > 450 m. These areas consist of regions located away from precipitating systems, which, in contrast, often have very shallow wake mixed layers ~ 100–200 m deep. These findings offer hope that *large-scale* numerical prediction models may be able to, even in highly convective regions, carry the mixed-layer depth as a predicted variable and take into account downdraft effects on the boundary layer in a manner similar to that described in this paper.

The model is applied to data for a composite of six large-scale tropical wave disturbances that passed the B-scale ship array during Phase III of GATE. The cloud-layer model of Johnson (1980) is used to determine a number of variables for the mixed-layer model: the mean subsidence velocity, cumulus mass detrainment rate at cloud base and

cloud downdraft mass flux at cloud base. Steady-state application of the mixed-layer model to the undisturbed wave ridge yields estimates of radiative jumps at the inversion. Average properties of downdraft air are specified from analysis of GATE boundary-layer observations in downdraft outflow wakes (Gaynor and Ropelewski, 1979).

Predictions for the composite wave demonstrate the important control by downdraft outflows on the mixed layer in the environment of precipitating systems. During periods of abundant deep convective activity, environmental subsidence (subsidence away from cumulus and mesoscale downdraft systems) is weak and yet the mixed layer does not grow without bound because of the inversion-strengthening effect of cool downdraft air outflow into the between-cloud region.

Due to the complexity of convection, it will probably be difficult to achieve a complete boundary-layer model applicable to all convective regimes in the GATE region. This study has been an attempt to simplify the problem by viewing the boundary layer in a large-scale sense; in essence, averaging over the area and life cycles of many convective systems. This approach does not suggest that smaller scale variations are unimportant: indeed, they may exert a profound influence on the initiation and subsequent development and decay of convective systems on the cumulus cloud and mesoscale. However, the results of this study indicate that large-scale models may not need to explicitly consider processes on time and space scales shorter and smaller than the mesoscale in order to obtain realistic predictions of the large-scale behavior of the mixed layer.

Acknowledgments. My appreciation is extended to Dr. Graeme Stephens, CSIRO, for helpful comments on radiative calculations (Section 4), to Dr. John Wyngaard, and an anonymous reviewer for several constructive criticisms. I would also like to thank Machel Sandfort for typing the manuscript. This research has been supported by the Division of Atmospheric Sciences, National Science Foundation under Grants ATM-8007462 and ATM-8015347.

REFERENCES

Arakawa, A., and W. H. Schubert, 1974: Interaction of a cumulus cloud ensemble with the large-scale environment. Part I. *J. Atmos. Sci.*, **31**, 674–701.

Barnes, G., G. D. Emmitt, B. Brümmer, M. A. Le Mone and S. Nicholls, 1980: The structure of a fair weather boundary layer based on the results of several measurement strategies. *Mon. Wea. Rev.*, **108**, 349–364.

Betts, A. K., 1973: Non-precipitating cumulus convection and its parameterization. *Quart. J. Roy. Meteor. Soc.*, **99**, 178–196.

——, 1974: Reply to comment on the paper "Non-precipitating cumulus convection and its parameterization." *Quart. J. Roy. Meteor. Soc.*, **100**, 469–471.

——, 1975: Parametric interpretation of trade-wind cumulus budget studies. *J. Atmos. Sci.*, **32**, 1934–1945.

——, 1976a: The thermodynamic transformation of the tropical subcloud layer by precipitation and downdrafts. *J. Atmos. Sci.*, **33**, 1008–1020.

——, 1976b: Modeling subcloud layer structure and interaction with a shallow cumulus layer. *J. Atmos. Sci.*, **33**, 2363–2382.

Brümmer, B., 1978: Mass and energy budgets of a 1 km high atmospheric box over the GATE C-Scale triangle during undisturbed and disturbed weather conditions. *J. Atmos. Sci.*, **35**, 997–1011.

Burroughs, W. J., 1979: The water dimer: a meteorologically important molecular species. *Weather*, **34**, 323–327.

Carson, D. J., 1973: The development of a dry inversion-capped convectively unstable boundary layer. *Quart. J. Roy. Meteor. Soc.*, **99**, 450–467.

Cho, H. R., 1977: Contributions of cumulus cloud life-cycle effects to the large-scale heat and moisture budget equations. *J. Atmos. Sci.*, **34**, 87–97.

Cox, S. K., and K. T. Griffith, 1979: Estimates of radiative divergence during Phase III of the GARP Atlantic Tropical Experiment. Part II: Analysis of Phase III results. *J. Atmos. Sci.*, **36**, 586–601.

Deardorff, J. W., 1974: Three-dimensional numerical study of the height and mean structure of a heated planetary boundary layer. *Bound.-Layer Meteor.*, **7**, 81–106.

——, 1979: Prediction of convective mixed-layer entrainment for realistic capping inversion structure. *J. Atmos. Sci.*, **36**, 424–436.

——, and J. A. Businger, 1980: Comments on "Marine stratocumulus convection. Part I: Governing equations and horizontally homogeneous solutions." *J. Atmos. Sci.*, **37**, 481–482.

Emmitt, G. D., 1978: Tropical cumulus interaction with and modification of the subcloud region. *J. Atmos. Sci.*, **35**, 1485–1502.

Esbensen, S., 1975: An analysis of subcloud-layer heat and moisture budgets in the western Atlantic trades. *J. Atmos. Sci.*, **32**, 1921–1933.

——, 1978: Bulk thermodynamic effects and properties of small tropical cumuli. *J. Atmos. Sci.*, **35**, 826–837.

Frank, W. M., 1979: Individual time period analyses over the GATE ship array. *Mon. Wea. Rev.*, **107**, 1600–1616.

Gaynor, J. E., and P. A. Mandics, 1978: Analysis of the tropical marine boundary layer during GATE using acoustic sounder data. *Mon. Wea. Rev.*, **106**, 223–232.

——, and C. F. Ropelewski, 1979: Analysis of the convectively modified GATE boundary layer using *in situ* and acoustic sounder data. *Mon. Wea. Rev.*, **107**, 985–993.

Houze, R. A., 1977: Structure and dynamics of a tropical squall-line system observed during GATE. *Mon. Wea. Rev.*, **105**, 1540–1567.

Jalickee, J. B., and C. F. Ropelewski, 1979: An objective analysis of the boundary-layer thermodynamic structure during GATE. Part I: Method. *Mon. Wea. Rev.*, **107**, 68–76.

Johnson, R. H., 1976: The role of convective-scale precipitation downdrafts in cumulus and synoptic-scale interactions. *J. Atmos. Sci.*, **33**, 1890–1910.

——, 1977: Effects of cumulus convection on the structure and growth of the mixed layer over south Florida. *Mon. Wea. Rev.*, **105**, 713–724.

——, 1978: Cumulus transports in a tropical wave composite for Phase III of GATE. *J. Atmos. Sci.*, **35**, 484–494.

——, 1980: Diagnosis of convective and mesoscale motions during Phase III of GATE. *J. Atmos. Sci.*, **37**, 733–753.

Leary, C. A., and R. A. Houze, 1979: The structure and evolution of convection in tropical cloud cluster. *J. Atmos. Sci.*, **36**, 437–457.

Lilly, D. K., 1968: Models of cloud-topped mixed layers under a strong inversion. *Quart. J. Roy. Meteor. Soc.*, **94**, 292–309.

Manton, M. J., 1978: Some effects of infrared radiation on the dynamics of the atmospheric boundary layer. *Pure Appl. Geophys.*, **116**, 1030–1048.

Nicholls, S., and M. LeMone, 1980: The fair weather boundary layer in GATE: The relationship of subcloud fluxes and structure to the distribution and enhancement of cumulus clouds. *J. Atmos. Sci.*, **37**, 2051–2067.

Nitta, T., 1975: Observational determination of cloud mass flux distributions. *J. Atmos. Sci.*, **32**, 73–91.

——, 1977: Response of cumulus updraft and downdraft to GATE A/B-scale motion systems. *J. Atmos. Sci.*, **34**, 1163–1186.

——, 1978: A diagnostic study of interaction of cumulus updrafts and downdrafts with large-scale motions in GATE. *J. Meteor. Soc. Japan*, **56**, 232–242.

Ooyama, K., 1971: A theory on parameterization of cumulus convection. *J. Meteor. Soc. Japan*, **49**, (Special Issue), 744–756.

Sarachik, E. S., 1974: The tropical mixed layer and cumulus parameterization. *J. Atmos. Sci.*, **31**, 2225–2230.

Stephens, G. L., 1976: An improved estimate of the IR cooling in the atmospheric window region. *J. Atmos. Sci.*, **33**, 806–809.

Tennekes, H., 1973: A model for the dynamics of the inversion above a convective boundary layer. *J. Atmos. Sci.*, **30**, 558–567.

Thompson, R. M., S. W. Payne, E. E. Recker and R. J. Reed, 1979: Structure and properties of synoptic-scale wave disturbances in the intertropical convergence zone of the eastern Atlantic. *J. Atmos. Sci.*, **36**, 53–72.

Zeman, O., and H. Tennekes, 1977: Parameterization of the turbulent energy budget at the top of the daytime atmospheric boundary layer. *J. Atmos. Sci.*, **34**, 111–123.

Zilitinkevich, S. S., 1975: Comments on "A model for the dynamics of the inversion above a convective boundary layer." *J. Atmos. Sci.*, **32**, 991–992.

Zipser, E. J., 1977: Mesoscale and convective-scale downdrafts as distinct components of squall-line circulation. *Mon. Wea. Rev.*, **105**, 1568–1589.